MOLECULAR
METABOLISM

Central NPFF signalling is critical in the regulation of glucose homeostasis

Lei Zhang [1,2,*,3], Julia Koller [1,2,3], Gopana Gopalasingam [1], Yue Qi [1], Herbert Herzog [1,2]

ABSTRACT

Objective: Neuropeptide FF (NPFF) group peptides belong to the evolutionary conserved RF-amide peptide family. While they have been assigned a role as pain modulators, their roles in other aspects of physiology have received much less attention. NPFF peptides and their receptor NPFFR2 have strong and localized expression within the dorsal vagal complex that has emerged as the key centre for regulating glucose homeostasis. Therefore, we investigated the role of the NPFF system in the control of glucose metabolism and the histochemical and molecular identities of NPFF and NPFFR2 neurons.

Methods: We examined glucose metabolism in $Npff^{-/-}$ and wild type (WT) mice using intraperitoneal (i.p.) glucose tolerance and insulin tolerance tests. Body composition and glucose tolerance was further examined in mice after 1-week and 3-week of high-fat diet (HFD). Using RNAScope double ISH, we investigated the neurochemical identity of NPFF and NPFFR2 neurons in the caudal brainstem, and the expression of receptors for peripheral factors in NPFF neurons.

Results: Lack of NPFF signalling in mice leads to improved glucose tolerance without significant impact on insulin excursion after the i.p. glucose challenge. In response to an i.p. bolus of insulin, $Npff^{-/-}$ mice have lower glucose excursions than WT mice, indicating an enhanced insulin action. Moreover, while HFD has rapid and potent detrimental effects on glucose tolerance, this diet-induced glucose intolerance is ameliorated in mice lacking NPFF signalling. This occurs in the absence of any significant impact of NPFF deletion on lean or fat masses, suggesting a direct effect of NPFF signalling on glucose metabolism. We further reveal that NPFF neurons in the subpostrema area (SubP) co-express receptors for peripheral factors involved in glucose homeostasis regulation such as insulin and GLP1. Furthermore, Npffr2 is expressed in the glutamatergic NPFF neurons in the SubP, and in cholinergic neurons of the dorsal motor nucleus of the vagus (DMV), indicating that central NPFF signalling is likely modulating vagal output to innervated peripheral tissues including those important for glucose metabolic control.

Conclusions: NPFF signalling plays an important role in the regulation of glucose metabolism. NPFF neurons in the SubP are likely to receive peripheral signals and mediate the control of whole-body glucose homeostasis via centrally vagal pathways. Targeting NPFF and NPFFR2 signalling may provide a new avenue for treating type 2 diabetes and obesity.

© 2022 The Author(s). Published by Elsevier GmbH. This is an open access article under the CC BY-NC-ND license (http://creativecommons.org/licenses/by-nc-nd/4.0/).

1. INTRODUCTION

Neuropeptide FF (NPFF) and neuropeptide AF (NPAF), which are processed out from the single prepropeptide encoding $Npff$ gene, are members of the large RFamide peptide family and designated as the NPFF group peptides [1,2]. Both, NPFF and NPAF act preferentially on the NPFFR2 receptor [3—5]. Originally identified as modulators of morphine-induced analgesia [6], NPFF group peptides and their receptor have since been shown to take part in other physiological functions, such as fluid homeostasis, energy metabolism and anxiety-like behaviours [7—12]. The expression of $Npff$ is restricted to the caudal brainstem and spinal cord in the mouse central nervous system [2,11]. In the caudal brainstem, $Npff$ is predominantly expressed in the subpostrema area (SubP), — the part of the nucleus of tractus

solitarius (NTS) immediately ventral to the area postrema (AP) [2,7,11]. The $Npff$ mRNA levels are influenced by energy status with negative energy balance induced by fasting leading to a strong increase in expression, while positive energy balance induced by high fat feeding has the opposite effect [7], implicating NPFF peptides in energy homeostasis control. Recently, it was shown that lack of NPFF signalling in mice leads to an altered oxidative fuel type selection during a fasting-refeeding challenge, while having little impact on feeding [11]. In comparison to NPFF, its high affinity receptor NPFFR2, shows a far wider expression throughout the brain; however also has a prominent expression in the dorsal motor nucleus of the vagus (DMV) [11,13]. The AP, NTS and DMV form the dorsal vagal complex (DVC) — an autonomic regulatory centre containing preganglionic parasympathetic neurons that control the subdiaphragmatic viscera [14,15].

[1]Neuroscience Division, Garvan Institute of Medical Research, St Vincent's Hospital, Darlinghurst, NSW, Australia [2]St. Vincent's Clinical Campus, School of Clinical Medicine, UNSW Medicine and Health, UNSW Sydney, NSW Australia

[3] Equal first authors.

*Corresponding author. Neuroscience Division, Garvan Institute of Medical Research, 384 Victoria Street, Darlinghurst, NSW 2010, Sydney, Australia. E-mail: l.zhang@garvan.org.au (L. Zhang).

Interestingly, recent studies have highlighted a pivotal role of DVC circuits in the control of glucose homeostasis by regulating parasympathetic efferent activity to corresponding organs, including the pancreas and liver [14,16,17]. The strong and localized expression of NPFF group peptides and its NPFFR2 receptor within structures of the DVC [11] also suggests a possible role of the NPFF system in glucose homeostatic regulation. Thus, in this study we examined the glucose and insulin tolerance in $Npff^{-/-}$ mice and further challenged them with a high-fat diet (HFD). Given the proximity of SubP NPFF neurons to the circumventricular organ AP and thus possible direct influence from circulating factors, we examined the expression of receptors for peripheral molecules on SubP NPFF neurons in mice.

2. MATERIALS AND METHODS

2.1. Animals
All research and animal care procedures were approved by the Garvan Institute/St. Vincent's Hospital Animal Ethics Committee and were performed in accordance with the Australian Code of Practice for the Care and Use of Animals for Scientific Purpose. Mice were housed under conditions of controlled temperature (22 °C for standard animal facility temperature, 29 °C for mouse thermoneutrality) and illumination (12-h light cycle, lights on at 07:00 h). All mice were fed a normal chow diet (6% fat, 23% protein, 51% carbohydrates, 5% fibre, 7% ash and 8% water with 13 MJ/kg; #27-mod-K1, Gordon's Speciality Stock Feeds, Yanderra, NSW, Australia) or a high-fat diet (HFD) (43% calories from fat, 17% calories from protein, 40% calories from carbohydrate and 20 MJ/kg; #SF03-020, Specialty Feeds, Glen Forrest, WA, Australia) and were given water *ad libitum*. The normal chow diet and HFD contained similar micronutrient and mineral compositions. The NPFF-deficient mice were obtained from Jackson Laboratory (B6N(Cg)-Npff$^{tm1.1(KOMP)Vlcg}$/J, $Npff^{-/-}$ for short). Mice details are available at Mouse Genome Informatics website (http://www.informatics.jax.org/reference/allele/MGI:5634708?typeFilter=Literature) and the International Mouse Phenotyping Consortium website (https://www.mousephenotype.org/data/genes/MGI:1891708#phenotypesTab). Littermate wild type (WT) and $Npff^{-/-}$ mice were studied.

2.2. Intraperitoneal glucose tolerance test
Male and female WT and $Npff^{-/-}$ mice at 10—11 weeks of age were examined. Food was removed from cage hoppers at 0900 h, and 6 h later a dose of glucose (1 g/kg body weight) was injected into the peritoneal cavity. Tail vein blood was collected at 0, 15, 30, 60 and 90 min after the glucose bolus injection for the determination of glucose concentrations using a glucometer (Accu-Chek® Go, Roche) and blood insulin levels using an ELISA kit from Crystal Chem (Crystal Chem, IL, USA) or serum insulin levels using a RIA kit (Millipore, Billerica, MA, USA). Glucose tolerance curves for glucose and insulin are presented as absolute values. Area under the glucose or insulin concentration curves between 0 and 90 min after glucose administration were calculated.

2.3. Intraperitoneal insulin tolerance test
Food was removed from cage hoppers at 1000 h, and 5 h later a dose of insulin (0.75 IU/kg for males, 1 IU/kg for females; Actrapid, Novo Nordisk, NSW Australia) was injected into the peritoneal cavity. Tail blood was collected at 0, 15, 30, 45, 60 and 75 min after the insulin bolus injection for the determination of glucose concentrations using a glucometer (Accu-Chek® Go, Roche). Area under the glucose concentration curves between 0 and 75 min after insulin injection

were calculated. Eleven-to-twelve weeks old WT and $Npff^{-/-}$ mice were examined.

2.4. High-fat diet study
A separate cohort of female WT and $Npff^{-/-}$ mice at 9—10 weeks of age were examined for basal glucose tolerance in response to an intraperitoneal glucose challenge as described above. Subsequently mice were fed on HFD and examined for glucose tolerance at 1 week and 3 weeks after the commencement of the HFD. One day prior the glucose tolerance test, mice were examined for whole-body lean and fat masses using EchoMRI™ system (Model 2016 E26-277-RM, EchoMRI LLC, TX USA).

2.5. Fasting-refeeding experiment
A cohort of female WT and $Npff^{-/-}$ mice at 14—15 weeks of age were evaluated for blood glucose and insulin responses to a fasting-refeeding challenge. Mice were group-housed with 2—3 mice per cage. Food was removed at 0900 h and given back at 0900 h the following day. Tail blood was taken prior to the food removal (pre-fast), and at the 0, 1, 3, and 24 h after the food representation for the determination of glucose concentrations using a glucometer (Accu-Chek® Go, Roche). Insulin levels were measured in tail blood samples at pre-fast, at 0 and 1 h after the food representation using an ELISA kit from Crystal Chem (Crystal Chem, IL, USA).

2.6. Serum assays
Serum insulin, free fatty acids and corticosterone levels were determined by the Insulin RIA kit (Millipore, Billerica, MA, USA), a NEFA HR kit using enzymatic colorimetric method (Wako Chemicals, Osaka, Japan), and a Corticosterone Double Antibody RIA kit (MP Biomedicals, LLC, Orangeburg, NY, USA), respectively.

2.7. *In situ* hybridization and quantification
We used RNAscope to visualize multiple cellular mRNA targets in fresh frozen tissues [18] — specifically the expression of *Npff* and *Npffr2* in adult mouse brains and their colocalization with *Slc32a1* (gene for GABA vesicular transporter, *Vgat*), *Slc17a6* (gene for vesicular glutamate transporter 2, *Vglut2*), or *Chat* (gene for choline acetyltransferase); the colocalization of *Npff* with insulin receptor (*Insr*), glucagon-like receptor-1 receptor (*Glp1r*), leptin receptor (*Lepr*), ghrelin receptor (also known as growth hormone secretagogue receptor, *Ghsr*), GDF15 receptor (GDNF family receptor alpha like, *Gfral*), neuropeptide Y (NPY) receptor Y1 (*Npy1r*), NPY receptor Y2 (*Npy2r*), NPY receptor Y4 (*Npy4r*). Coronal brain sections (25 μm) were cut on a cryostat and thaw-mounted on Superfrost® slides (Menzel-Glaser, Braunschweig, Germany), and dual or triple labelled with RNAScope® probes targeting the mRNA of *Npff* (#479901-C2), *Npffr2* (#410171), *Slc32a1* (#319191-C3), *Slc17a6* (#319171-C3), *Chat* (#408731-C2), *Insr* (#401011), *Glp1r* (#418851), *Lepr* (#402731), *Ghsr* (#426141), *Gfral* (#417021), *Npy1r* (#427021), *Npy2r* (#315951), *Npy4r* (#313551) using RNAscope® 2.5 Duplex Detection Kit or RNAscope® Multiplex Fluorescent Detection Reagents following manufacturer's protocol (Advanced Cell Diagnostics, Inc.). Pictures were taken using a DM 6000 Power Mosaic microscope (Leica, Germany) for brightfield images and a DM 5500 microscope (Leica, Germany) for fluorescent images. The number of neurons that express *Npff*, and neurons co-express *Npff* with *Vglut2*, *Vgat*, *Npffr2*, *Insr*, *Glp1r*, *Lepr*, *Ghsr*, *Gfral*, *Npy1r*, *Npy2r* or *Npy4r* were counted in the subpostrema area (SubP, between Bregma level −7.76 mm and −7.32 mm). Two to three sections from the RNAscope fluorescent assay were chosen for each brain and two to three brains were used for each probe combination.

The photomicrogrpahs of the regions were acquired (Leica DM5500), and the percentage of NPFF-expressing neurons that co-express the gene of interest was obtained from each side of the SubP.

2.8. Statistical analyses
All data are expressed as means ± SEM. Statistical difference between two groups were assessed by t-test. Difference between genotypes over a time-course with multiple measurements was evaluated by repeated-measures ANOVA followed by Tukey's or Sidak's post-hoc analysis where appropriate. Analyses were conducted using PRISM, version 9.0 (GraphPad Software Inc., San Diego, CA, USA). Statistical significance was defined as $p < 0.05$.

3. RESULTS

3.1. Improved glucose tolerance and insulin action in $Npff^{-/-}$ mice
In order to investigate whether NPFF signalling is involved in glucose homeostasis, we performed glucose tolerance tests in WT and $Npff^{-/-}$ mice. WT and $Npff^{-/-}$ had comparable body weight (18.91 ± 0.31 g and 18.87 ± 0.41 g for female WT and $Npff^{-/-}$, respectively; NS by t-test. 25.14 ± 0.55 g and 24.74 ± g for male WT and $Npff^{-/-}$, respectively; NS by t-test; Supplementary Figure 1), consistent with

previous report [11]. After an i.p. bolus of glucose (1 g/kg), both male and female $Npff^{-/-}$ mice exhibited significantly lower blood glucose excursions compared to their gender-matched WT mice (Figure 1A, C). The resultant area under the glucose curves were significantly reduced in $Npff^{-/-}$ versus WT mice for both genders (Figure 1B, D), indicating an improved glucose tolerance. The insulin excursions after the i.p. glucose challenge did not significantly differ between genotypes for both genders (Figure 1E, G), leading to a comparable area under the insulin curves between $Npff^{-/-}$ and WT mice (Figure 1F, H). The improved glucose tolerance (Figure 1A–D) without significant change in insulin excursion (Figure 1E–H) suggest an enhanced insulin action in $Npff^{-/-}$ mice. To examine this, we conducted an insulin tolerance test. In response to an i.p. insulin challenge, both male and female $Npff^{-/-}$ mice showed lower glucose levels compared to their gender-matched WT counterparts, significantly so from 15 min onwards after the challenge (Figure 1I, K), which is in support of an increased insulin action in $Npff^{-/-}$ mice. The area under the glucose curve over the 75 min examination period showed a strong trend towards decreasing in $Npff^{-/-}$ versus WT mice for both genders ($p = 0.07$) (Figure 1J, L). Together, these data showing an improved glucose tolerance and insulin action in $Npff^{-/-}$ mice suggest an important role of NPFF signalling in the regulation of glucose homeostasis.
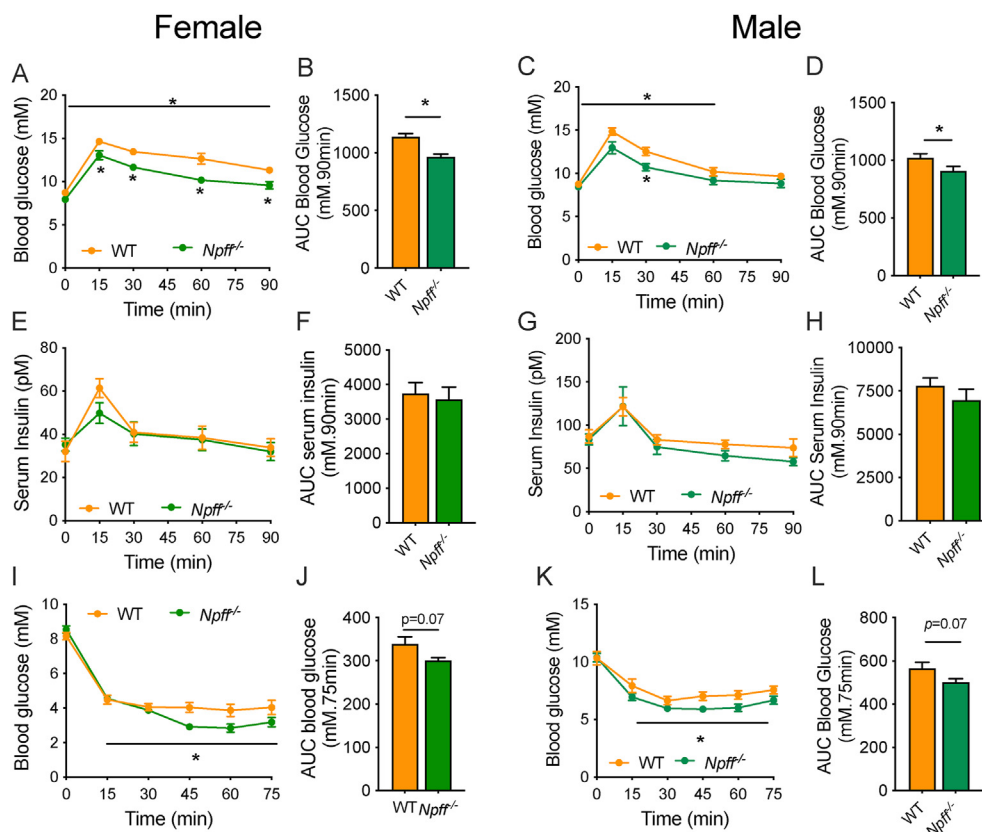
Figure 1: Improved glucose tolerance and insulin action in $Npff^{-/-}$ mice. Blood glucose excursions (A) and area under the glucose curves (B) after an intraperitoneal (i.p.) bolus of glucose (1 g/kg) in female mice (n = 14 and 13 for WT and $Npff^{-/-}$, respectively). Blood glucose excursions (C) and area under the glucose curves (D) after an i.p. bolus of glucose (1 g/kg) in male mice (n = 11 for WT and $Npff^{-/-}$). Serum insulin excursions (E) and area under the insulin curves (F) after i.p. glucose bolus in female mice (n = 12 and 10 for WT and $Npff^{-/-}$, respectively). Serum insulin excursions (G) and area under the insulin curves (H) after i.p. glucose bolus in male mice (n = 11 for WT and $Npff^{-/-}$). Blood glucose excursions after an i.p. bolus of insulin (1U/kg) (I) and resultant area under the glucose curves (J) in female mice (n = 9 for WT and $Npff^{-/-}$). Blood glucose excursions after an i.p. bolus of insulin (0.75U/kg) (K) and area under the glucose curves in male mice (n = 13 and 12 for WT and $Npff^{-/-}$, respectively). Mice at 10–12 weeks of age were used. Data are shown as mean ± SEM. Data were analysed by t-test or repeated-measure ANOVA with Sidak method for multiple comparison correction. *$p < 0.05$ between genotypes or as indicated by bars. Bars in (A), (C), (I) and (K) indicate comparisons between genotypes over indicated period.

3.2. Ameliorated diet-induced glucose intolerance in $Npff^{-/-}$ mice

Having seen an improved glucose tolerance in $Npff^{-/-}$ mice on chow (Figure 1), we examined whether $Npff^{-/-}$ mice are protected from diet-induced glucose intolerance. We conducted glucose tolerance tests in a group of mice at basal chow condition, and at 1 and 3 weeks on HFD. Since male and female $Npff^{-/-}$ mice show the same improvement in glucose tolerance on chow (Figure 1), we performed these experiments using only female mice. HFD significantly increased body weight in both WT and $Npff^{-/-}$ mice after 1 week and further so after 3 weeks (Figure 2A). Whole-body fat mass significantly increased in both WT and $Npff^{-/-}$ mice from 1-week onwards (Figure 2B), while whole-body lean mass remained unaltered over the monitoring period (Figure 2C). There was no significant genotype difference in body weight (Figure 2A), fat (Figure 2B) or lean (Figure 2C) masses at any of the examined time points, indicating a comparable impact of HFD on body composition between WT and $Npff^{-/-}$ mice. Consistent with the previous cohort (Figure 1), $Npff^{-/-}$ mice under baseline chow condition responded to the i.p. glucose challenge with a significantly lower glucose excursion (Figure 2D) and area under the glucose curve (Figure 2G) compared to WT mice. This occurred with a trend of lower insulin excursion (Figure 2H) compared to those in WT mice, in line with the enhanced insulin action. When fed on HFD, $Npff^{-/-}$ mice displayed comparable glucose (Figure 2E) and insulin excursions (Figure 2I) to those of WT mice at 1-week HFD, however showed significantly improved glucose tolerance (Figure 2F, G) after 3-week HFD, suggesting that lack of NPFF signalling provides protection against diet-induced glucose intolerance. Insulin levels after the glucose bolus were comparable between $Npff^{-/-}$ and WT mice at both 1 and 3 weeks on HFD (Figure 2I—K).

Having seen a regulatory role of NPFF on glucose metabolism during a high glucose influx, like the i.p. glucose bolus, we examined blood glucose responses in female $Npff^{-/-}$ and WT mice in response a 24-hour fast where glucose influx is zero, and subsequent refeeding. WT and $Npff^{-/-}$ mice are shown to have comparable food intake after a 24-hour fast [11]. Blood glucose levels showed a drop after the 24-hour fast and a gradual return to baseline after 24-hour refeed without significant genotype differences (Supplementary Figure 2A). In addition, circulating insulin levels were comparable between genotypes at baseline, after 24-hour fast and at 1 h after the food presentation (Supplementary Figure 2B). Moreover, serum levels of free fatty acids and corticosterone after 24-hour fasting were comparable between female WT and $Npff^{-/-}$ mice (Supplementary Figure 2C and D).

3.3. Central NPFF signalling control glucose homeostasis

We [11] and others [19] have shown that the NPFFR2, — the cognate receptor for NPFF, is absent in mouse liver and skeletal muscle, — two important tissues involved in the glucose metabolism. To investigate whether NPFF could have direct actions on other glucose-regulatory peripheral tissues, we examined the $Npffr2$ mRNA expression in the mouse pancreas by RNAscope and observed little $Npffr2$ mRNA expression (Figure 3A). The expression of $Npffr2$ has been reported in the inguinal white adipose tissue macrophages [20]. However, since activation of Npffr2 signalling in these white adipose tissue macrophages was reported to improve glucose metabolism [20], the improved glucose tolerance observed in the $Npff^{-/-}$ mice is likely to be contributed by central mechanisms.

3.4. NPFF and NPFFR2 neurons in the DVC are glutamatergic and cholinergic, respectively

To gain insights into the central mechanisms via which NPFF signalling may impact glucose metabolism, we examined the neurochemical identity of NPFF and NPFFR2 neurons in the dorsal vagal complex (DVC) by RNAScope. About 95% of all $Npff$-expressing neurons in the SubP co-expressed the vesicular glutamate transport $Vglut2$ (Figure 3B-(i), E), indicating that NPFF is released primarily from excitatory glutamatergic neurons. Interestingly, in over 90% of NPFF neurons investigated, there were also a few copies of $Npffr2$ mRNA present (Figure 3B-(i), E), pointing to the possibility that NPFFR2 may also act as an auto-receptor to exert feedback inhibition on NPFF neurons. There was little colocalization ($\sim$10%) between $Npff$ and the vesicular GABA transporter $Vgat$ (Figure 3C-(i), E).

With regards to $Npffr2$ mRNA that is heavily expressed in the DMV, we saw little co-localization with $Vglut2$ (Figure 3B-(ii)) or $Vgat$ (Figure 3C-(ii)). Thus, we performed RNAScope with dual labelling of $Npffr2$ and choline acetyltransferase ($Chat$) — the enzyme responsible for the synthesis of the neurotransmitter acetylcholine. $Npffr2$-expressing neurons in the DMV were heavily co-stained for $Chat$ mRNA in a chromogenic assay (Figure 3D-(a)). To better separate the staining for each probe we further performed a fluorescent assay and observed clear co-localization of $Npffr2$ with $Chat$ (Figure 3D-(b)), demonstrating that NPFFR2 neurons in the DMV are primarily cholinergic neurons and thus likely to be involved in modulating parasympathetic output to tissues including those involved in glucose metabolic regulation.

3.5. NPFF neurons in the SubP co-express receptors for peripheral factors involved in the regulation of glucose metabolism

Since the SubP NPFF neurons are in proximity to the area postrema, a circumventricular organ, we asked whether these NPFF neurons could be influenced directly by peripheral circulating factors involved in the regulation of glucose metabolism and energy homeostasis. For this we examined the NPFF neurons for their expression of receptors for several key peripheral signal molecules including insulin, glucagon-like peptide-1 (GLP1), ghrelin, leptin, growth differentiation factor 15 (GDF15), peptide YY (PYY), PYY3-36, and pancreatic polypeptide (PP). The SubP NPFF neurons show highest colocalization with insulin receptor ($Insr$, $\sim$40%) (Figure 4A, I), followed by GLP1 receptor ($Glp1r$, $\sim$24%) (Figure 4B, I), receptor for GDF15 ($Gfral$, 23%) (Figure 4E, I), receptor for PYY and PYY3-36 ($Npy1r$ and $Npy2r$, $\sim$18% and 13%, respectively) (Figure 4F, G, I), leptin receptor ($Lepr$, 11%) (Figure 4C, I), ghrelin receptor ($Ghsr$, $\sim$8.5%) (Figure 4D, I) and receptor for PP ($Npy4r$, 7.6%) (Figure 4H, I). These data suggest that SubP NPFF neurons receive direct input from peripheral factors to regulate glucose and energy homeostasis with insulin and GLP1 being the most prominent ones in the control of glucose metabolism.

4. DISCUSSION

This is the first study to show that central NPFF signalling is directly influencing glucose homeostasis control since lack of NPFF in mice improves glucose tolerance and ameliorates diet-induced impairment in glucose tolerance. Moreover, the absence of any impact of NPFF deletion on body weight, whole-body lean or fat masses confirms this direct effect of NPFF signalling on glucose metabolism. Mechanistically, NPFF signalling regulates glucose metabolism primarily via impacting on insulin action since the improvement of glucose tolerance in $Npff^{-/-}$ mice occurred in the absence of changes in insulin excursion and $Npff^{-/-}$ mice also exhibited lower glucose excursions during an insulin tolerance test. Moreover, the lack of any significant expression of Npffr2 receptors in peripheral glucose responsive tissues suggests that central mechanisms are likely to be responsible for this action. This is further supported by the observation that specific receptors for peripheral circulating factors involved in glucose
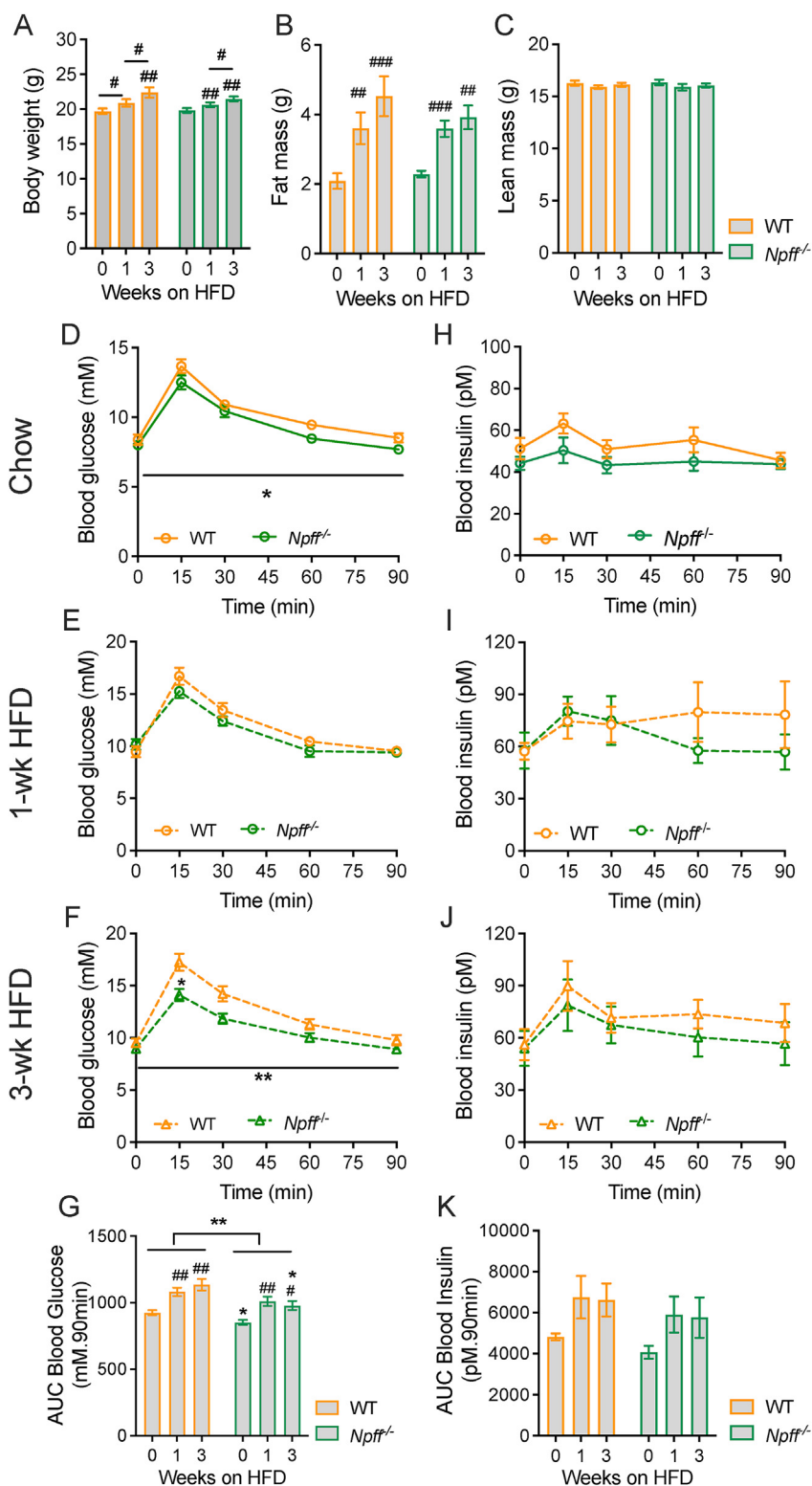
Figure 2: Ameliorated diet-induced glucose intolerance in *Npff*^−/− mice. Body weight (A), whole-body fat mass (B) and lean mass (C) in WT and *Npff*^−/− mice at baseline chow, after 1-week and 3-week of high-fat diet (HFD) feeding (n = 11 for WT and *Npff*^−/−). Blood glucose excursions in WT and *Npff*^−/− mice after an intraperitoneal bolus of glucose (1 g/kg) at baseline chow (D), after 1-week HFD (E) and 3-week HFD (F) (n = 11 for WT, n = 10−11 for *Npff*^−/−). (G) Area under the glucose curves for (D−F). Insulin excursions in WT and *Npff*^−/− mice after an intraperitoneal bolus of glucose (1 g/kg) at baseline chow (H), after 1-week HFD (I) and 3-week HFD (J) (n = 5−6 for WT, n = 4 for *Npff*^−/−). (K) Area under the insulin curves for (H−J). Female mice at 10 weeks of age were used. Data are shown as mean ± SEM. Data were analysed by two-way repeated measures ANOVA and subsequent multiple comparisons were corrected using Sidak and Tukey method for between- and within-subject comparisons, respectively. #$p < 0.05$, ##$p < 0.01$, ###$p < 0.001$ versus 0-week HFD of the same genotype or as indicated by bars (A, B, G). *$p < 0.05$, **$p < 0.01$ between genotypes over the time-course as indicated by bars (D, F), between genotypes of the same treatment (G) and between groups by repeated measures ANOVA indicated by bracket in (G).
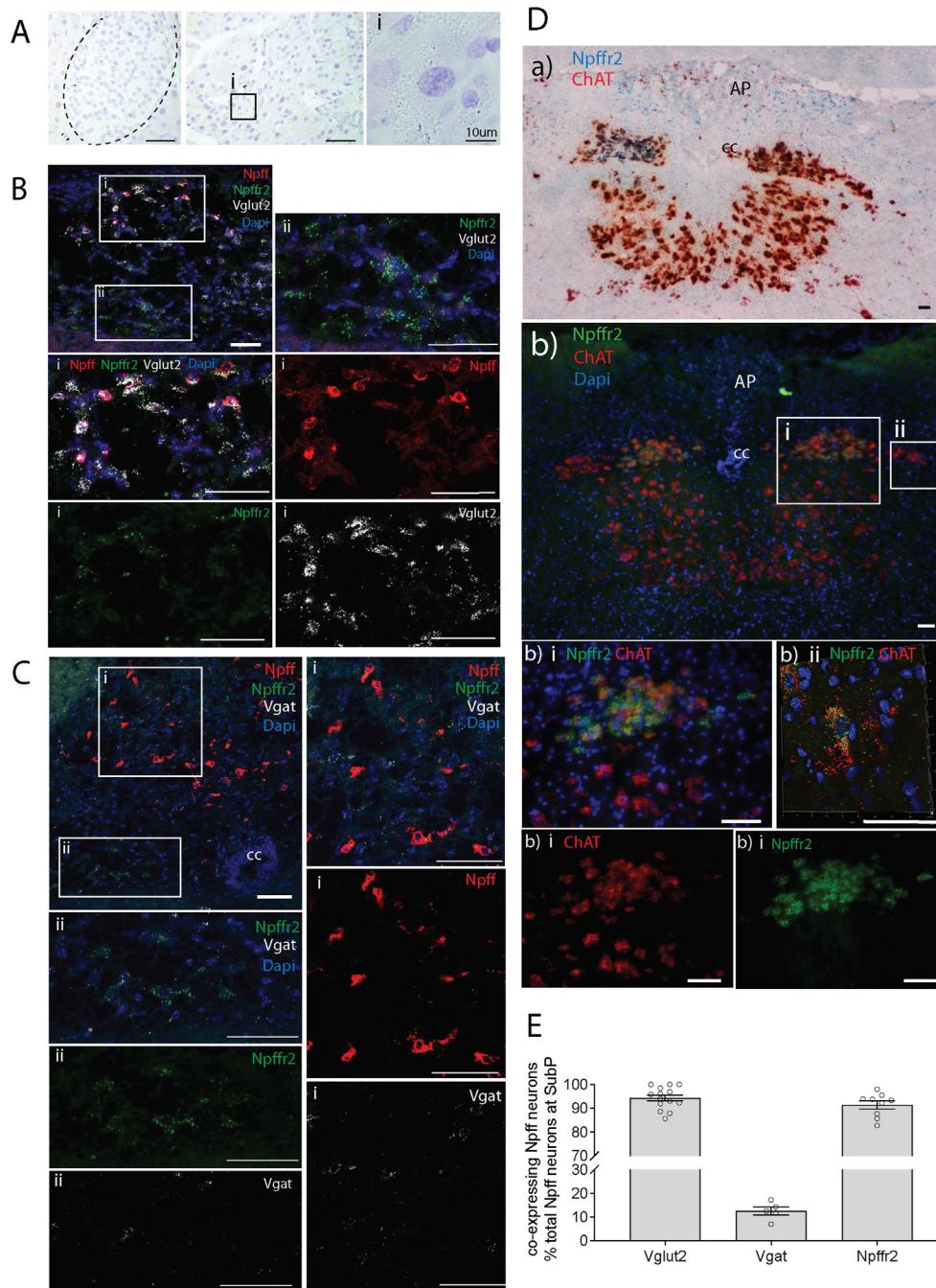
Figure 3: The neurochemical identities of NPFF and NPFFR2 neurons. Representative image of RNAscope chromogenic analysis of *Npffr2* mRNA expression in mouse pancreatic tissue (A), Sections were counterstained with haematoxylin. *Npffr2* mRNA expression is indicated by blue dots. (B) Expression of *Npffr2, Npff* and *Vglut2* mRNA in the subpostrema area (i) and dorsal motor nucleus of the vagus (ii). Red, green and white signal indicate the expression of *Npffr2, Npff* and *Vglut2*, respectively. Sections were counterstained with dapi (purple). (C) Expression of *Npffr2, Npff* and *Vgat* in subpostrema area (i) and dorsal motor nucleus of the vagus (ii). Red, green and white signals indicate the expression of *Npff, Npffr2,* and *Vgat*, respectively. Sections were counterstained with dapi (purple). (D) Co-expression of *Npffr2* and *Chat* in the dorsal motor nucleus by chromogenic assay (a) and fluorescent assay (b). In a), red and blue signals indicate the expression of *Chat* and *Npffr2*, respectively; section was counterstained with haematoxylin. In b), red and green signals indicate the expression of *Chat* and *Npffr2*, respectively; section was counterstained with dapi (purple). (E) Percentage of NPFF neurons in the subpostrema area that co-express *Vglut2, Vgat* or *Npffr2*. Data are mean ± SEM. cc: central canal; Vglut2: vesicular glutamate transporter 2 (*Slc17a6*); Vgat: GABA vesicular transporter (*Slc32a1*); ChAT: choline acetyltransferase; SubP: subpostrema area. Scale bars = 50 μm unless indicated otherwise.

homeostatic control, such as insulin and GLP1, are found to be expressed on NPFF neurons in the SubP. We also demonstrate that Npffr2 is co-expressed in glutamatergic NPFF neurons in the SubP, which together with their inhibitory signalling function [3,4] suggests an auto-inhibitory feedback function in these neurons. Finally, NPFFR2 neurons in the DVC are predominantly of cholinergic nature, indicating
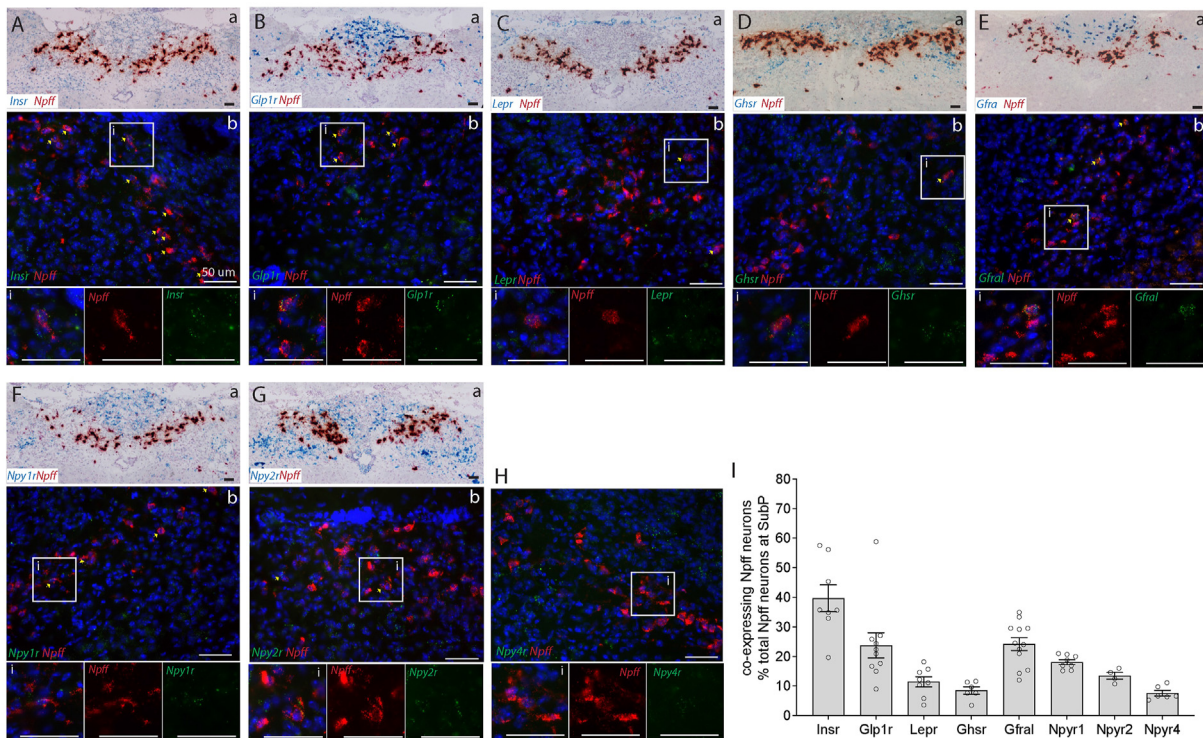
Figure 4: NPFF neurons in the subpostrema area co-express receptors for peripheral factors. Representative images of RNAscope analysis of co-expression of *Npff* with insulin receptor (*Insr*) (A), glucagon-like receptor-1 receptor (*Glp1r*) (B), leptin receptor (*Lepr*) (C), ghrelin receptor (growth hormone secretagogue receptor, *Ghsr*) (D), GDF15 receptor (GDNF family receptor alpha like, *Gfral*) (E), neuropeptide Y (NPY) receptor Y1 (*Npy1r*) (F), NPY receptor Y2 (*Npy2r*) (G), NPY receptor Y4 (*Npy4r*) (H). a) in (A—G) chromogenic assay where *Npff* mRNA was stained in red, indicated receptor mRNA was stained in blue; sections were counterstained with haematoxylin. b) in (A—G) and H) fluorescent RNAscope assay where *Npff* mRNA was stained in red, indicated receptor mRNA was stained in green; sections were counterstained with dapi (purple); yellow arrows indicate neurons co-expressing *Npff* and the indicated receptor. Scale bar = 50 μm. I) Quantification of percentage NPFF-expression neurons in the subpostrema area (SubP) that co-express receptors indicated on x-axis. Data are mean ± SEM.

that NPFF signalling may involve modulating vagal output to innervated peripheral tissues including those important for glucose metabolic control.

The SubP NPFF neurons are in a strategic location to mediate the function of circulating factors from the periphery. For one, the SubP is part of the NTS which is a major gateway for visceral afferent information [21]. For another, the proximity of the SubP to the circumventricular organ AP makes the access to peripheral factors possible [22]. The latter is supported by findings from this study showing that SubP NPFF neurons express a myriad of receptors for peripheral factors involved in glucose and energy metabolic control. Among the examined receptors, the insulin receptor is the most prominent followed by the GLP1 receptor. Both insulin and GLP1 are well-known players in the regulation of glucose metabolism that involves their central actions [23—26]. The expression of their receptors on SubP NPFF neurons suggest that SubP NPFF neurons may form part of the central regulator loops via which insulin and/or GLP1 control glucose metabolism. It's worth to note that in addition to peripherally produced GLP1 from the enteroendocrine L cells in the gut, GLP1 produced from the preproglucogan neurons in the hindbrain also participates in the regulation of glucose metabolism [27,28]. Moreover, both insulin and GLP1 are also known to regulate feeding and energy metabolism via actions on the brain [24,29,30]. Interestingly, mice that lack NPFF signalling, while exhibiting altered oxidative fuel selection in response to a fasting-refeeding challenge, are WT-like with regards to feeding behaviour or energy expenditure [11]. Thus, it seems possible that a

direct action of insulin and/or GLP1 on SubP NPFF neurons may be more specific for the regulation of glucose metabolism rather than controlling feeding. Curiously, the SubP NPFF neurons have moderate colocalization with Gfral (~23%), — a receptor for GDF15 that has implications in anorexia through nausea and emesis [31]. Whether SubP NPFF neuron participate in the GDF15/Gfral system-induced anorexia responses may warrant future investigation.

We hypothesize that one central pathway through which the NPFF system exerts effects on glucose metabolism may be via modulating parasympathetic activity to peripheral responsive organs. This is based on 1) the predominant expression of *Npff* and *Npffr2* within the structure of the DCV and 2) the colocalization of *Npffr2* with *Chat* in DMV — indicative of NPFFR2 neurons being cholinergic neurons that control parasympathetic output. Considering the inhibitory nature of NPFFR2 signalling [3,4], lack of Npff would lead to a disinhibition of those cholinergic DMV neurons previously under the inhibition of NPFFR2 signalling and likely leading to an increased parasympathetic output. Increased parasympathetic activity has been shown to inhibit hepatic gluconeogenesis and improves whole-body glucose clearance [14,16,17]. This is also consistent with the observed effect of HFD reducing *Npff* expression [7], likely being an attempted to release this NPFFR2 induced brake on DMV neurons.

Our results also show that there is little or no *Npffr2* expression in the mouse pancreas, consistent with findings from rats [3]. Together with previous reports on very little *Npffr2* expression on other insulin-sensitive tissues including the skeletal muscle, liver, or abdominal

white adipose tissue [3,11], a direct action of NPFF signalling on these tissues seems unlikely. Interestingly, however, *Npffr2* is reported to be expressed in inguinal adipose tissue macrophages and their activation by NPFF leads to M2 activation and increased adipose tissue macrophage self-renewal, which contribute to an improved glucose metabolism [20]. In this regard, our results showing an improved glucose tolerance in the absence of NPFF may suggest that the centrally mediated effects of NPFF signalling on glucose metabolism may outweigh effects via its peripheral actions. Taken together, targeting NPFF and NPFFR2 signalling may provide a new avenue for treating type 2 diabetes and obesity.

ACKNOWLEDGEMENTS

CONFLICT OF INTEREST

The authors have declared that no conflict of interest exists.

APPENDIX A.   SUPPLEMENTARY DATA

Supplementary data to this article can be found online at https://doi.org/10.1016/j.molmet.2022.101525.

REFERENCES

[1] Perry, S.J., Yi-Kung Huang, E., Cronk, D., Bagust, J., Sharma, R., Walker, R.J., et al., 1997. A human gene encoding morphine modulating peptides related to NPFF and FMRFamide. FEBS Letters 409(3):426—430.

[2] Vilim, F.S., Aarnisalo, A.A., Nieminen, M.L., Lintunen, M., Karlstedt, K., Kontinen, V.K., et al., 1999. Gene for pain modulatory neuropeptide NPFF: induction in spinal cord by noxious stimuli. Molecular Pharmacology 55(5): 804—811.

[3] Bonini, J.A., Jones, K.A., Adham, N., Forray, C., Artymyshyn, R., Durkin, M.M., et al., 2000. Identification and characterization of two G protein-coupled receptors for neuropeptide FF. Journal of Biological Chemistry 275(50):39324—39331.

[4] Elshourbagy, N.A., Ames, R.S., Fitzgerald, L.R., Foley, J.J., Chambers, J.K., Szekeres, P.G., et al., 2000. Receptor for the pain modulatory neuropeptides FF and AF is an orphan G protein-coupled receptor. Journal of Biological Chemistry 275(34):25965—25971.

[5] Mollereau, C., Mazarguil, H., Marcus, D., Quelven, I., Kotani, M., Lannoy, V., et al., 2002. Pharmacological characterization of human NPFF(1) and NPFF(2) receptors expressed in CHO cells by using NPY Y(1) receptor antagonists. European Journal of Pharmacology 451(3):245—256.

[6] Ayachi, S., Simonin, F., 2014. Involvement of mammalian RF-amide peptides and their receptors in the modulation of nociception in rodents. Frontiers in Endocrinology 5:158.

[7] Zhang, L., Ip, C.K., Lee, I.J., Qi, Y., Reed, F., Karl, T., et al., 2018. Diet-induced adaptive thermogenesis requires neuropeptide FF receptor-2 signalling. Nature Communications 9(1):4722.

[8] Kalliomaki, M.L., Panula, P., 2004. Neuropeptide FF, but not prolactin-releasing peptide, mRNA is differentially regulated in the hypothalamic and medullary neurons after salt loading. Neuroscience 124(1):81—87.

[9] Arima, H., Murase, T., Kondo, K., Iwasaki, Y., Oiso, Y., 1996. Centrally administered neuropeptide FF inhibits arginine vasopressin release in conscious rats. Endocrinology 137(5):1523—1529.

[10] Yokoi, H., Arima, H., Kondo, K., Murase, T., Iwasaki, Y., Yang, H.Y., et al., 1998. Antiserum against neuropeptide FF augments vasopressin release in conscious rats. Peptides 19(2):393—395.

[11] Zhang, L., Koller, J., Ip, C.K., Gopalasingam, G., Bajaj, N., Lee, N.J., et al., 2021. Lack of neuropeptide FF signalling in mice leads to reduced repetitive behavior, altered drinking behavior, and fuel type selection. The FASEB Journal 35(11):e21980.

[12] Koller, J., Herzog, H., Zhang, L., 2021. The distribution of neuropeptide FF and neuropeptide VF in central and peripheral tissues and their role in energy homeostasis control. Neuropeptides 90:102198.

[13] Liu, Q., Guan, X.M., Martin, W.J., McDonald, T.P., Clements, M.K., Jiang, Q., et al., 2001. Identification and characterization of novel mammalian neuropeptide FF-like peptides that attenuate morphine-induced antinociception. Journal of Biological Chemistry 276(40):36961—36969.

[14] Zsombok, A., Smith, B.N., 2009. Plasticity of central autonomic neural circuits in diabetes. Biochimica et Biophysica Acta 1792(5):423—431.

[15] Young, A.A., 2012. Brainstem sensing of meal-related signals in energy homeostasis. Neuropharmacology 63(1):31—45.

[16] Pocai, A., Obici, S., Schwartz, G.J., Rossetti, L., 2005. A brain-liver circuit regulates glucose homeostasis. Cell Metabolism 1(1):53—61.

[17] Meyers, E.E., Kronemberger, A., Lira, V., Rahmouni, K., Stauss, H.M., 2016. Contrasting effects of afferent and efferent vagal nerve stimulation on insulin secretion and blood glucose regulation. Physiological Reports 4(4).

[18] Wang, F., Flanagan, J., Su, N., Wang, L., Bui, S., Allisssa, N., et al., 2012. RNAscope: a novel in situ RNA analysis platform for formalin-fixed, paraffin-embedded tissues. Journal of Molecular Diagnostics 14(1):22—29.

[19] Leon, S., Velasco, I., Vazquez, M.J., Barroso, A., Beiroa, D., Heras, V., et al., 2018. Sex-biased physiological roles of NPFF1R, the canonical receptor of RFRP-3, in food intake and metabolic homeostasis revealed by its congenital ablation in mice. Metabolism 87:87—97.

[20] Waqas, S.F.H., Hoang, A.C., Lin, Y.T., Ampem, G., Azegrouz, H., Balogh, L., et al., 2017. Neuropeptide FF increases M2 activation and self-renewal of adipose tissue macrophages. Journal of Clinical Investigation 127(7):2842—2854.

[21] Andresen, M.C., Kunze, D.L., 1994. Nucleus tractus solitarius—gateway to neural circulatory control. Annual Review of Physiology 56:93—116.

[22] van der Kooy, D., Koda, L.Y., 1983. Organization of the projections of a circumventricular organ: the area postrema in the rat. Journal of Comparative Neurology 219(3):328—338.

[23] Filippi, B.M., Yang, C.S., Tang, C., Lam, T.K., 2012. Insulin activates Erk1/2 signaling in the dorsal vagal complex to inhibit glucose production. Cell Metabolism 16(4):500—510.

[24] Fujikawa, T., 2021. Central regulation of glucose metabolism in an insulin-dependent and -independent manner. Journal of Neuroendocrinology 33(4): e12941.

[25] Williams, D.L., 2009. Minireview: finding the sweet spot: peripheral versus central glucagon-like peptide 1 action in feeding and glucose homeostasis. Endocrinology 150(7):2997—3001.

[26] Sandoval, D.A., Bagnol, D., Woods, S.C., D'Alessio, D.A., Seeley, R.J., 2008. Arcuate glucagon-like peptide 1 receptors regulate glucose homeostasis but not food intake. Diabetes 57(8):2046—2054.

[27] Jessen, L., Smith, E.P., Ulrich-Lai, Y., Herman, J.P., Seeley, R.J., Sandoval, D., et al., 2017. Central nervous system GLP-1 receptors regulate islet hormone secretion and glucose homeostasis in male rats. Endocrinology 158(7):2124—2133.

[28] Shi, X., Chacko, S., Li, F., Li, D., Burrin, D., Chan, L., et al., 2017. Acute activation of GLP-1-expressing neurons promotes glucose homeostasis and insulin sensitivity. Molecular Metabolism 6(11):1350—1359.

[29] Loh, K., Zhang, L., Brandon, A., Wang, Q., Begg, D., Qi, Y., et al., 2017. Insulin controls food intake and energy balance via NPY neurons. Molecular Metabolism 6(6):574—584. https://doi.org/10.1016/j.molmet.2017.03.013.eCollection.Jun.

[30] Fortin, S.M., Lipsky, R.K., Lhamo, R., Chen, J., Kim, E., Borner, T., et al., 2020. GABA neurons in the nucleus tractus solitarius express GLP-1 receptors and mediate anorectic effects of liraglutide in rats. Science Translational Medicine 12(533).

[31] Borner, T., Shaulson, E.D., Ghidewon, M.Y., Barnett, A.B., Horn, C.C., Doyle, R.P., et al., 2020. GDF15 induces anorexia through nausea and emesis. Cell Metabolism 31(2):351—362 e5.